Synthesis, X-Ray Structure, Hirschfield surfaces Analysis and DFT Computations of new Schiff bases

Abdelghani Madani *[1], Anis Bouchama[2], Abdelkader Hellal[3]

[1]Laboratory of Electrochemistry and Materials, Department of Process Engineering, Faculty of Technology, Setif 1 University-Ferhat Abbas. Algeria.

Email: abdelghani.madani@univ-setif.dz;

[2]Laboratory of Electrochemistry of Molecular Materials and Complexes. Department of Process Engineering, Faculty of Technology, Setif 1 University-Ferhat Abbas. Algeria.

Email: aniswdf0107@gmail.com

[3*]Laboratory of Electrochemistry of Molecular Materials and Complexes. Department of Process Engineering, Faculty of Technology, Setif 1 University-Ferhat Abbas. Algeria.

Email: abdelkader.hellal@univ-setif.dz

*Corresponding author, Email: abdelghani.madani@univ-setif.dz;

Abstract

The novel Schiff base compound named as 3-[(1*Z*)-*N*-(4'-aminobiphenyl-4-yl)ethanimidoyl]-2-hydroxy-6-methyl-4*H*-pyran-4-one is synthesized by the chemical reaction of benzidine and acid déhydroacitic acid (DHA) in absolute ethanol under reflux condition, and the structure of the titled compound is verified and characterized by infrared, ultraviolet-visible (UV-vis) spectroscopies and the single-crystal X-ray diffraction technique. The compound crystallized in the monoclinic system, space group C 2/c, with the following unit cell parameters a=14.175(2), b=5.736(2) and c=21.150(2) A° and α =90°, β=107.5(6)°, ɣ=90° and Z=4 , V= 1602.45(10) ($Å^3$), T = 170(2)K, The final R1 was 0.0482 ($I > 2\sigma(I)$) and wR2 was 0.1395 (all data). The structure for the $C_{20}H_{18}N_2O_3$ was examined using Hirschfield topology analysis and Density Functional Theory (DFT) calculations a detailed study based on B3LYP/6-311G (d, p). The graphical tools based on Hirschfield surfaces and two-dimensional (2D) fingerprint plots have proven useful for visualize and analyze intermolecular interactions in polymorphs of molecular crystals. The optimized geometry, global reactivity descriptors, and HOMO-LUMO orbitals of the molecule were computed using the DFT-B3LYP method and discussed to evaluate the chemical reactivity and charge distribution on the molecule. The theoretical bond lengths and angles for the $C_{20}H_{18}N_2O_3$ wereobtained by using the B3LYP level of density function theory (DFT) with B3LYP /6-311G (*d*, *p*) basis sets. These results showed very good agreement with the experimental X-ray values.

Keywords: Benzidine, Schiff base, Crystal structure, Hirschfield surfaces, DFT**.**

1. Introduction

Aldehydes and ketones are being used as main products in most organic synthesis thanks to the significant reactivity of their functional group C=O. Indeed, the dissimilarity of their C=O electronegativity is the basis that explains such large interest. The afford property mentioned, i.e. the important reactivity of the aldehyds and ketones functional group C=O allows many chemical experimentations on their function. In the same frame work, it is to mention that Schiff basis are

compounds of general formula R1R2C=NR3 in which the roots R1, R2 and R3 may be alkyls, cycloalkyles or aromatics nucleic groups. They have been first synthesized by the German chemist *Hugo Schiff* in 1864 [1], for such they are called thus, i.e. "Schiff bases". Atoms suppliers of electron pairs such N, O, S that ligand Schiff bases' contains find their use in several applications. A large number of its derivatives are used in materials science such as solar shell [2], optical switching [3], third order non-linear optics (NLO) [4], electrochemical sensing [5].They are famous for their biological application as antibacterial [6], antifungal, antiviral, anti-HIV [7], antioxidant [8], anti-inflammatory agents [9], anticonvulsant [10],antihypertensive activity [11]and anti-HIV activities [12].anti-protozoal[13], anti-cancer agents [14], The objective of this study is to synthesize new Schiff bases, the $C_{20}H_{18}N_2O_3$, are characterized by single-crystal X-ray diffraction and infrared. The title compound was examined using Hirschfield topology and analysis intermolecular interactions in polymorphs of molecular crystals, optimized geometry of molecular properties such equilibrium energy, frontier orbital, energy gap, molecular electrostatic potential energy gap, dipole moment, polarizability are calculated and discussed bay density functional theory, (DFT), level employing the basis set 6-31G(d,p)

2. Materials and Methods

2.1. Experimental

All of the chemical substances used in this research were acquired from Sigma-Aldrich and used without additional purification. UV–vis spectra were obtained using a JASCO V-650 UV–Vis spectrophotometer with quartz cells of 1 cm path length in dimethylformamide (DMF) between 200 and 800 nm. FT-IR spectra were obtained using a JASCO 4200 spectrometer between 4000 and 400 cm^{-1}. X-ray diffraction were obtained using aBruker–Nonius Kappa-CCD diffractometer with monochromatic Mo-Kα radiation (λ = 0.71073 Å)

2.2. Synthesis of Schiff base compound

The compoound Schiff base was synthesized by reaction in a 1:1 molar ratio of the 4,4'-diaminobiphenyl (3.0g, 1.6mmol)ande acid déhydroacitic acid (0.3g, 1.6mmol) in absolute ethanol for 4h at 55 °C (Scheme 1). The crystalline product was obtained by slow evaporation at room temperature. The crystalline product that formed was filtered and washed with cold ethanol and dried over anhydrous silica gel. *3*-[(1Z)-N(4'-aminobiphenyl-4yl)ethanimidoyl]-2-hydroy-6-methyl-4Hpyran-4 one: FT IR, υ= 1595 cm-1 (C=N);υ=1665 cm-1 (C=O); υ=1043cm-1 (C-O-C); υ= 1356 cm-1 (OH). UV-Vis (DMF, λ_{max}= 374,05nm (n→π* (C=C)) of the aromatic ring and λ_{max}= 285.92 nm (n→π*or π→σ* azomethine group (-CH=N-)). Solubility: Soluble in MeOH, EtOH and DMSO, Yield (62%). *Mp*: 250 252°C. $C_{20}H_{18}N_2O_3$. Mol.Wt=334.35g/mol.

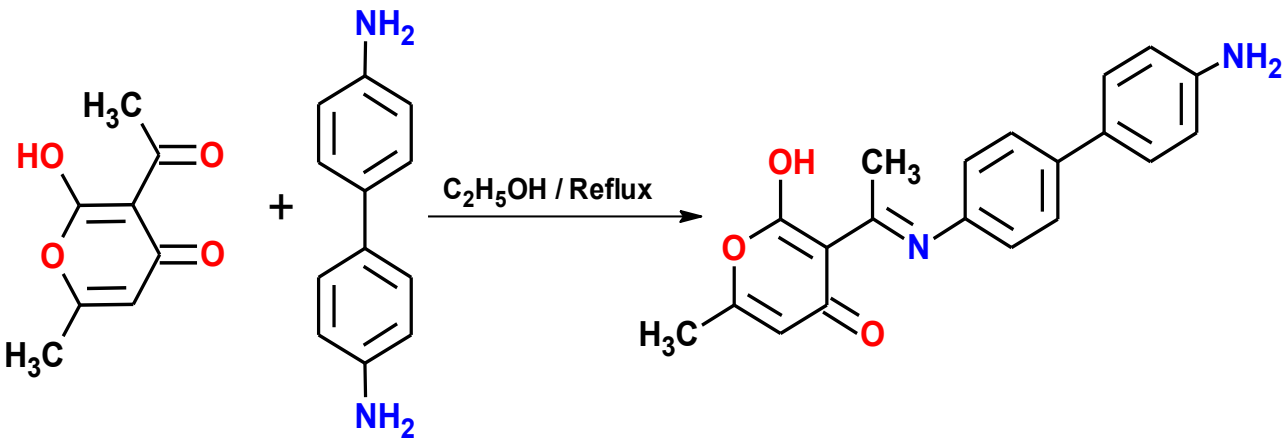

Scheme.1. Synthesis of Schiff base compound.

2.3. Crystallography and Hirschfield surfaces calculations

A suitable single crystal of the compound $C_{20}H_{18}N_2O_3$ with dimensions of 0.15× 0.13 × 0.10 mm was used for data collection .X-ray diffraction study was done on Bruker–Nonius X8 ApexIIdiffractometer using monochromatic Mo-Kα radiation (λ = 0.71073 Å).The structure of $C_{20}H_{18}N_2O_3$was determined based on 56852 reflections, of which 4362 reflections were considered observable under the conservation criterion I >2σ(I). The reflections were measured in the angular domain $2.96 \leq \theta \leq 29.28$. The molecular structure was resolved through direct methods using the SHELXT packet [15], and refined by full matrix least squares method against F^2 by SHELXL package[29]. All hydrogen atoms were allocated geometrically and placed isotropically. The molecular geometry was calculated using the WinGX[16] and graphic illustrations were performed using the software Diamond [17].The crystallographic detail of the compound is summarized in (Table 1).The resulting structure has been the subject of a legal deposition to Cambridge Crystallographic Data Center (CCDC) under CCDC code 2009187 and DOI: 10.5517/ccdc.csd.cc25fqhv..To analyze 3D Hirshfeld surfaces and 2D fingerprint plots associated with molecular interactionCrystal Explorer 17.5 program [18] was used, for which the information file (CIF) was used as input. The molecular Hirshfeld surface of compound (BB) was generated using a standard (high) surface resolution with the $3Dd_{norm}$,d_e, d_i,surfaces, the shape index, curvatureandfragment patch. The surfaces were shown to be transparent to allowvisualization of the molecular moiety in a similar orientation for all of the structures around which they were calculated.

2.4. Theoretical analysis

All calculations were carried out using DFT calculations at the B3LYP/6-311G(d,p) level of theory with 6-311G(d, p) basis set.Geometry optimization, an important issue in molecular mechanics, was performed as the first task of the computational work for the synthesized molecules. It requires in particular the sensitivity of the interaction energy with respect to the change of the molecule's shape which is in general induced by the movement of the nuclei positions. The molecular structure, vibrational frequencies and energies of the optimized geometries of SB1 and SB2 were calculated employing the DFT [19] method using Gaussian 09 [20] program package employing 6-311G(d,p) basis set based on Becke's three parameters (local, non-local, Hartree-Fock) hybrid exchange functional with Lee-Yang-Parr correlation functional (B3LYP) [21-23]. The basis set 6-311G(d,p) augmented by 'd' polarization functions on heavy atoms and 'p' polarization functions on hydrogen atoms as well as diffuse functions for both hydrogen and heavy atoms were used [24-25].

3. Results and Discussion

3.1. Chemistry

The3-[(1*Z*)-*N*-(4'-aminobiphenyl-4-yl)ethanimidoyl]-2-hydroxy-6-methyl-4*H*-pyran-4-one is synthesized by a *one-pot in situ* condensation of one equivalent of benzidine and acid déhydroacitic acid (DHA) in absolute ethanol under reflux condition, for a reaction time of 10 h (Scheme 1). The product thus obtained, was filtered off, washed with methanol and ether, recrystallized in methanol and dried in vacuo over fused $CaCl_2$. A pure white powder with a conversion of 57% and a melting point of 252-254°C was obtained. The structure of 3-[(1*Z*)-*N*-(4'-aminobiphenyl-4-yl)ethanimidoyl]-2-hydroxy-6-methyl-4*H*-pyran-4-onewas confirmed by spectroscopic methods such as infrared (FTIR), ultraviolet-visible (UV-vis) and by X-ray diffraction technique. The FTIR (KBr, 4000–400 cm^{-1}) spectrum gives several characteristic bands. The broad band at 1665 cm^{-1} indicates the presence of a carbonyl group in the molecule. The presence of the ant symmetric vibration and symmetric vibration of the $-NH_2$ amino group[26], expected at 3379 and 3218 cm^{-1}, indicates the condensations of acid déhydroacitic acid (DHA)carbonyl groups with the "$-NH_2$" of 4, 4'diaminobiphenyl. A strong band due to the C=N (azomethine) moiety is pointed at 1577 cm^{-1}[27], a broad centered band at 3350 cm^{-1} is assigned to –OH stretching vibration along with two deformation bands near 1100 and 1170 cm^{-1}. Also a strong band appears in the range of 1694 cm^{-1} in the conpound is assigned to the C=O group of the pyran ring. The Schiff bases synthesized exist in tautomeric form, mainly as imine-enol form.[28-30].The electronic spectrum of the product displayed, an intense band at 285.92 nm, which is attributed to the (n→π*) transition associated with the azomethine group (CH=N-), another band at 374.05 nm, which is due to the (n→π*) transition in the C=C of various aromatic ring.

3.2. X-ray crystal structure description

The molecular structure of 3-[(1*Z*)-*N*-(4'-aminobiphenyl-4-yl)ethanimidoyl]-2-hydroxy-6-methyl-4*H*-pyran-4-one was solved by direct methods using SHELXT package. The geometry of the molecule was calculated using the WinGX and PLATON software, the crystallographic data are summarized in Table 1.

Cristallographic Data	
Empiric Formula $C_{20}H_{18}N_2O_3$	Cristallin System : Monoclinic
Espace group p 21/n	Temperature (K) 170(2)
a(Å) = 13.982(5)	Longueur d'onde Mo Kα (Å) λ =0.71073
b(Å) = 5.7434(2)	molecularweight (g mol^{-1}) 331.16
c(Å) = 20.99 (7)	Yellowcolor
α(°) = 90	Z= 4
β(°) = 108.09(10)	V(Å^3) = 1602.45(10)
γ(°) = 90	
Acquisition des données et affinement structural	
Domaine de θ (°) 2.96- 29.288	Reflexions$I$> 2σ(I) 4362
Reflexions 56852	R $_{indices}$ (tout data) 0.0724
Reflexionsindependantes 4362	Parametersnumber246
R1 [F^2>2σ(F^2)] 0.0482	$\Delta\rho_{min}$(e Å-3) -0.585
wR2 [F^2>2σ(F^2)] 0.1395	$\Delta\rho_{max}$(e Å-3) 0.704
Goodness GoF :1.040	

Table 1. Crystal data and structure refinement for compound

.The compound was crystallized in the monoclinic system, space group p 21/n with the following unit cell parameters a =13.982(5) Å, b =5.7434(2) Å, c =20.99 (7) Å and β=108.09(10)° and Z = 4 , V=1602.45(10) (Å^3), T = 170(2) K, The final R1 was 0.0482 (I > 2σ(I)) and wR2 was 0.1395 (all data) without the presence of any solvent molecule.The molecular structure of 3-[(1*Z*)-*N*-(4'-aminobiphenyl-4-yl)ethanimidoyl]-2-hydroxy-6-methyl-4*H*-pyran-4- is shown in Figure1.With displacement ellipsoids plotted at 50% probability level.

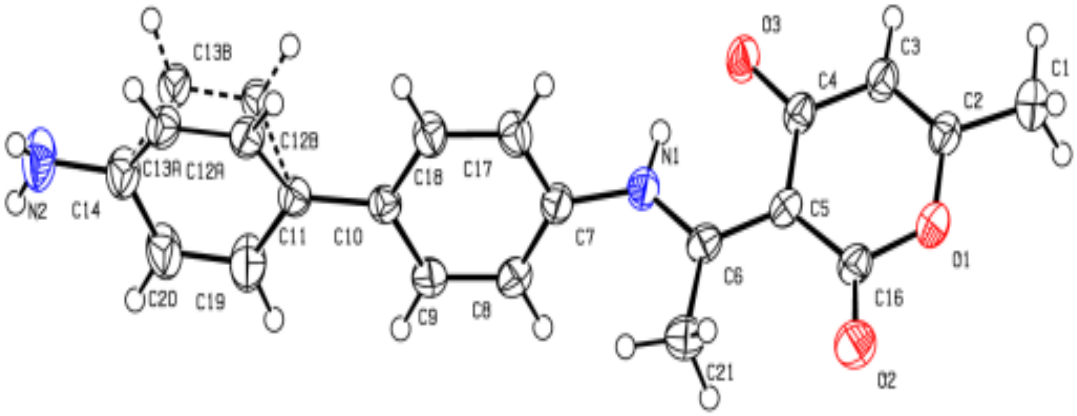

Figure1.ORTEP representation of compound displacement ellipsoids are drawn at the 50% probability level.

The compound $C_{20}H_{18}N_2O_3$ crystallizes in the space group P21/n of the monoclinic system with an asymmetric unit consisting of three rings in the form of the two aromatic rings of the benzidine unit defined by the atoms C7,C6, C8, C10,C18, C17 / C11,C16, C20, C14,C13, C12, and the third dehydroacitic acid defined by the atoms C2,C3, C4, C5,O1, C19, the different cycles of the molecule have distances and angles almost normal. The molecular structure of $C_{20}H_{18}N_2O_3$ can be influenced by intramolecular hydrogenbonding; O—H••• N contact. In the structure of $C_{20}H_{18}N_2O_3$, the N atom is protonated and the C=N imine bond configuration is E in the molecule. The C4=O3 bond length is 1.259(2) Å, which confirms that it is a double bond. The asymmetric unit consists ofan entity of formula $[C_{20}H_{18}N_2O_3]$ located in a general position as shown in Figure 2. This structure canbe described as follows: the entities of the compound derivative develop in the plane (101) to form chainsFigure.2. The junctions between the molecules within the same chain as well as the cohesion between twoadjacent chains are ensured by means of intra and intermolecular hydrogen bonds. The examination of intra and intermolecular interactions therefore reveals, as we have just indicated, the existence of intra and intermolecular hydrogen bridges involving the oxygen atoms and nitrogen atoms of the adjacent molecules. All of these interactions therefore ensure three-dimensional cohesion of the structures.

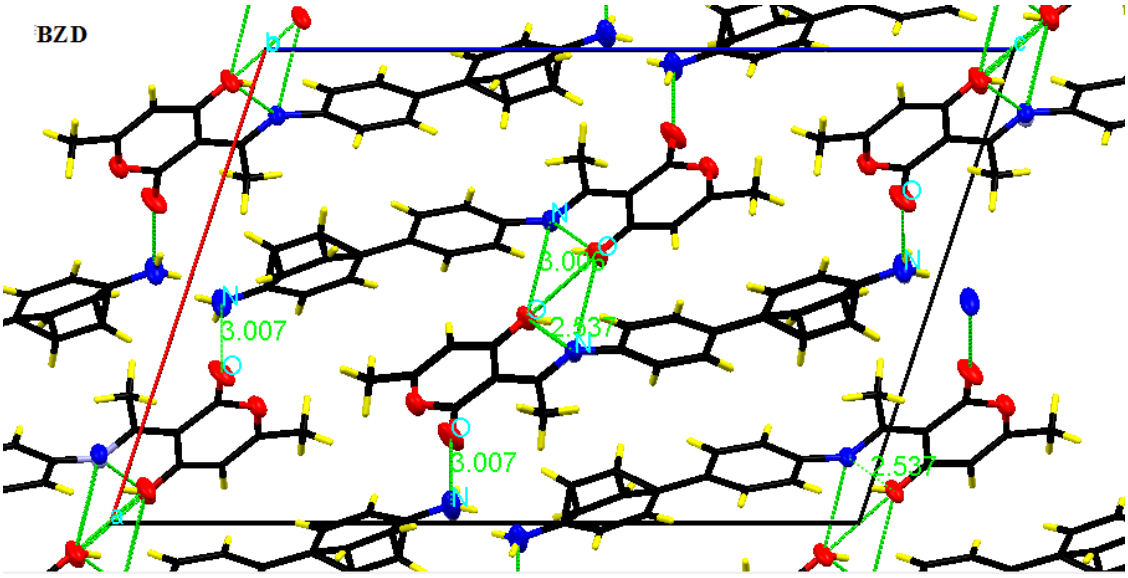

Figure 2. Representation of intra- and inter- interactions in the compound.

3.3. Hirshfeld surface and 2D fingerprints

The Hirshfeld surface is mapped over a denim ranging from -0.674 to 2.4484 Å marking three different colored regions on the surface: red regions representing stronger interactions with contacts less than van der Waals distance, blue regions with contacts above the distance van der Waals and white regions with inter/intra-molecular contacts equal to the distance van der Waals. The surface properties d_i and $d_e$are mapped in the ranges 0.7202 to 2.4484 Å and 0.7203 to 2.4463Å, respectively.The other surface properties like shape index, surface curvedness, and fragment patch are plotted between -1 to 1, -4 to 0.4, and 0 to 13, respectively (Figure 3).

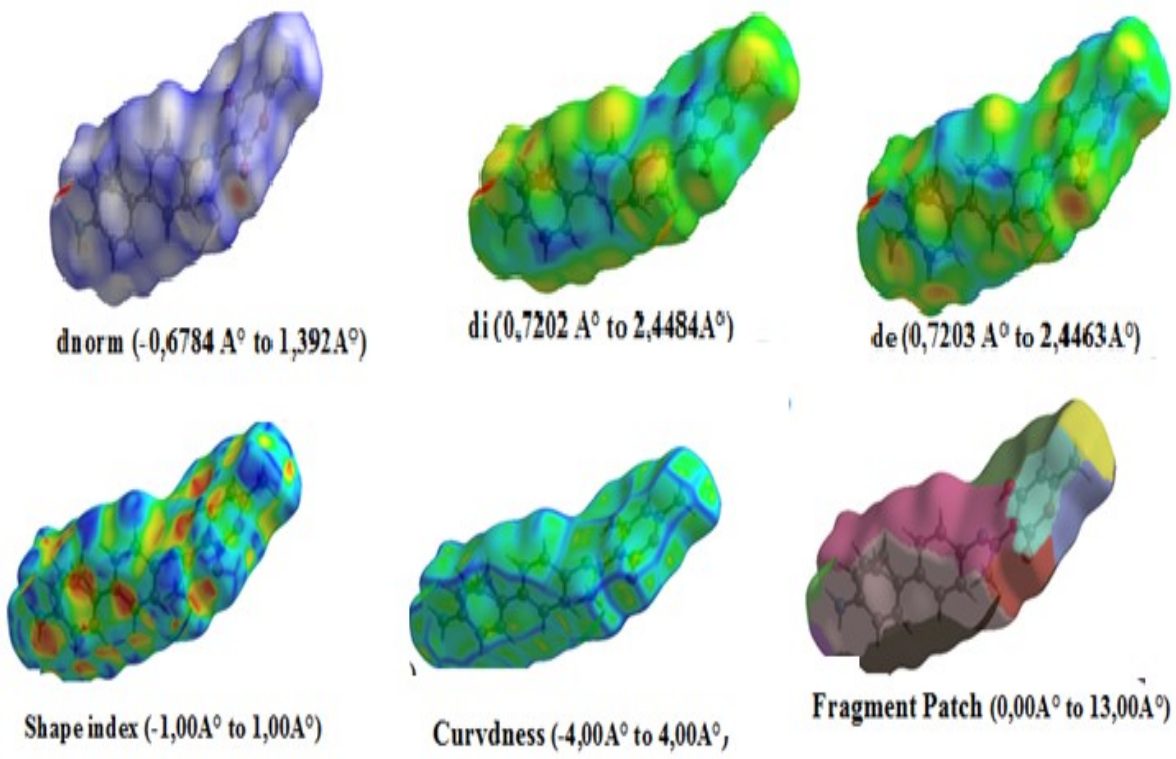

Figure 3. Hirschfield surface: *d* norm, di, de, Shape index, Curvedness andfragment Patch of compound.

The 2D fingerprint plot of $C_{20}H_{18}N_2O_3$is demonstrated in Figure 4 and the intermolecular interactions in $C_{20}H_{18}N_2O_3$ are mainly constituted by H···H, C···H, O···H, C···O, C···N, H···N and C···C contacts [31-32].The shortest contacts correspond to the very close H···H contacts, showing a sharp spike centred near a (de+ di) sum of 2.26 Å. The decomposition of the fingerprint plot shows that H···H contacts occupy 46.1 % of the total Hirshfeld surface area, C···H contacts = 31.9 %, O···H = 16,6% and H···N, C···C, contacts contribute only 1.7 % and 0.4 %, respectively, to the total Hirshfeld surface area Figure 4.

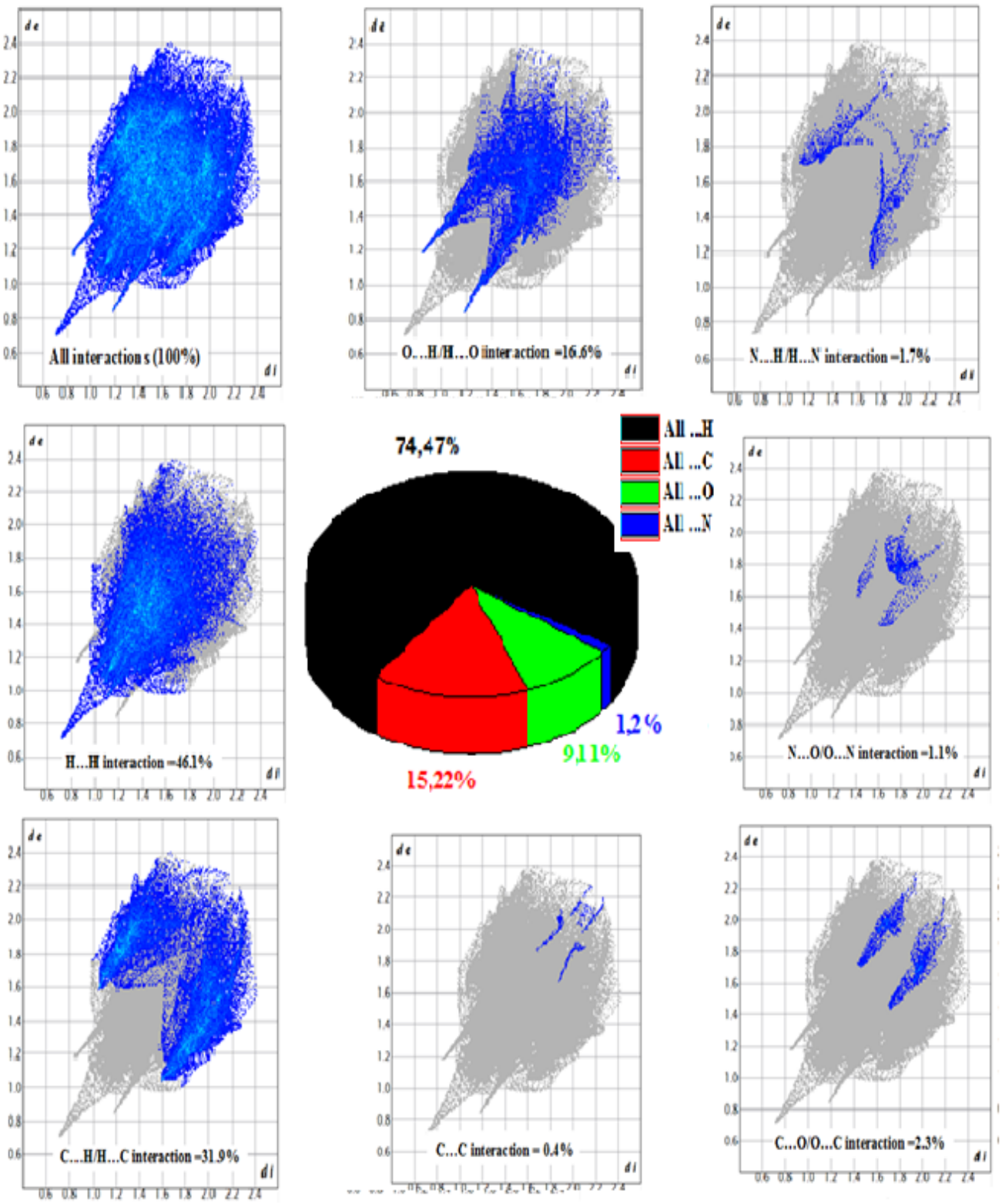

Figure 4. Two-dimensional fingerprint plot for all interactions and individual interactions in crystal packing and the percentage contributions of the interaction of all the atoms present inside the HS to an atom outside the HS

3.4.DFT studies

The optimized molecular structure is calculated using DFT theory at B3LYP/6-311G level of basis set by Gaussian 09 program package along with atom numbering scheme as illustrated in figure 5

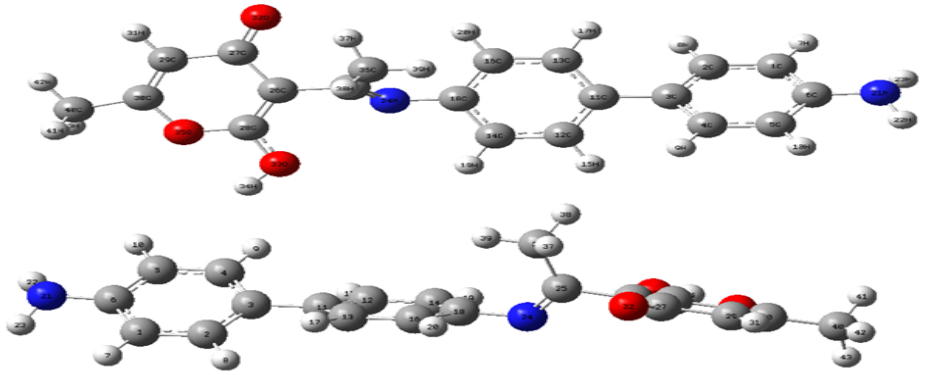

Figure.5. The optimized molecular structure of compound using DFT (B3LYP)/6- 31G(d,p)

The optimized parameters of $C_{20}H_{18}N_2O_3$is calculated by B3LPY/6-31G (d,p) is listed in Table 2. All the bond lengths and bond angles in heterocyclic rings are in the common range. The "C–C" and "C–O" bond distances are found to be in the range from1.3688A°-1.3556A° , 1.2029-1.4265 A° ,while for "C=N", these values are 1.2737Å. All the "C-CC" angles lay

between 117.53° to 121.61o. All the dihedral angles are between -179°and +179° showing the non-planar structure.

bond	Bond lengths (A)	bond	Bond angles (θ)	bond	Dihedral angles (θ)
C1-C2	1.3881	C2-C1-C6	120.7631	C6-C1-C2-C3	0.059
C1-C6	1.4026	C2-C1-H7	119.7537	C6-C1-C2-H8	178.6574
C1-H7	1.0791	C6-C1-H7	119.4776	H7-C1-C2-C3	-179.0734
C2-C3	1.4031	C1-C2-C3	121.8193	H7-C1-C2-H8	-0.475
C2-H8	1.0844	C1-C2-H8	118.7564	C2-C1-C6-C5	-0.0699
C3-C4	1.4032	C3-C2-H8	119.4096	C2-C1-C6-N21	-177.0693
C3-C11	1.482	C2-C3-C4	116.8949	H7-C1-C6-C5	179.0648
C4-C5	1.388	C2-C3-C11	121.5374	H7-C1-C6-N21	2.0655
C14-C18	1.4014	C3-C11-C12	121.3431	C4-C3-C11-C12	36.2033
C14-H19	1.084	C3-C11-C13	121.3634	C4-C3-C11-C13	-143.0961
C16-C18	1.4009	C12-C11-C13	117.2901	C3-C4-C5-C6	-0.1677
C16-H20	1.0836	C11-C12-C14	121.6105	C3-C4-C5-H10	-179.5777
C18-C25	1.406	C11-C12-H15	119.4782	H9-C4-C5-C6	178.1222
N21-H22	1.0095	C14-C12-H15	118.8961	H9-C4-C5-H10	-1.2878
N21-H23	1.0095	C11-C13-C16	121.5092	C4-C5-C6-C1	0.1231
N24-C25	1.2737	C11-C13-H17	119.3897	C4-C5-C6-N21	177.1211
C25-C26	1.5046	C16-C13-H17	119.056	H10-C5-C6-C1	179.5343

Table.2. Selected optimized parameters of $C_{20}H_{18}N_2O$by B3LYP/6-31G(d,p) basis set

The HOMO and LUMO energy calculated by B3LYP/6-31G(d,p) method for both molecules is shown below. Increased LUMO energy level and decreased HOMO energy level results in higher HOMOLUMO gap. Higher HOMO-LUMO gap corresponds to higher kinetic stability, thus, lower chemical reactivity [33-35]. That is, a small interval between HOMO-LUMO implies low kinetic stability and high chemical reactivity, as it is energetically favorable to add electrons to a LUMO and to extract electrons from a HOMO. The HOMO-LUMO energy of the compound **is** 0.1316 ua. Among many others, the energy difference between HOMO and LUMO has been used to predict the activity and intramolecular charge transfer in organic molecules with conjugated π bonds [36-37]. The 3D plots of the frontier orbital are HOMO and LUMO, for the both molecules are as shown in Figure6, the green and red solid regions represent the MOs with completely opposite phases. The positive phase of the molecule is represented in red color and negative phase in green color.

.

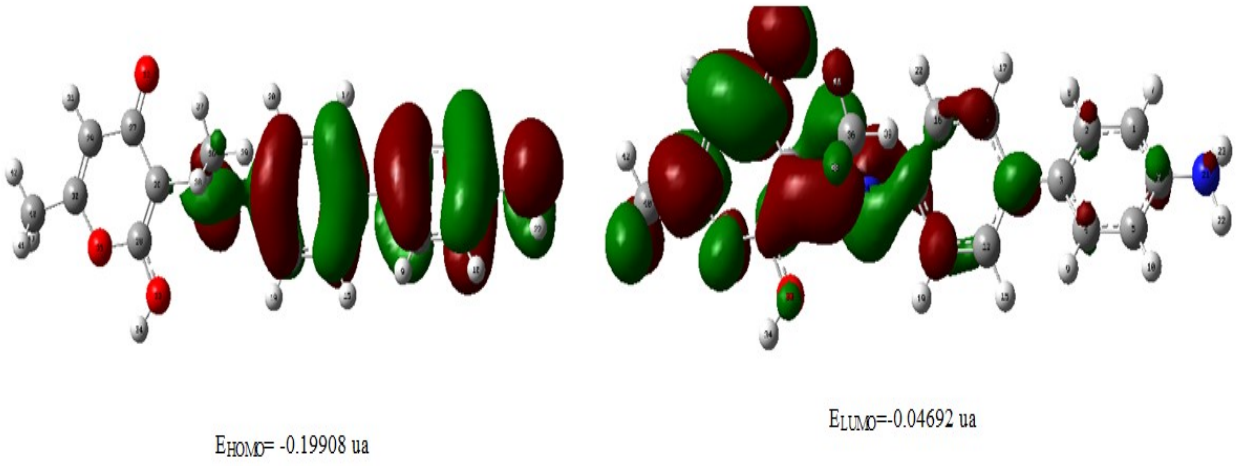

Figure.6. The optimized molecular structure and orbitals HOMO-LUMO

The quantum chemical properties led us to know how to find the energy states of the molecules. Chemical bonds are a source of energy and the movement of molecules in the space is kinetic energy. The vibrations and rotations of molecules is another source of chemical energy along with the chemical reaction, which is a rearrangement of atoms. Density functional theory has been successful in providing insights into the chemical reactivity and selectivity in terms of global parameters, like electronegativity, hardness, and softness [38].The chemical potential provides a global reactivity index and is related to charge transfer from a system of higher chemical potential to one of lower chemical potential. Electronegativity is the power to attract electrons and it is related directly to all above properties mentioned. All these properties are defined as follows [39-40]. The electrophilicity index is a measure of decrease in total energy during electron sharing [41]. The ionization potential (IP) and electron affinity (EA)can be calculated from the HOMO and the LUMO energies.The HOMO-LUMO energy gap, electronegativity, electrophilicity index, and chemical hardness and softness values of compound**is** listed in **Table 3:**

Energies	Gas	Aqueous
E_{tot}(a.u)	-1108.4226	-1108.43260
E_{HOMO} a.u	-0,19084	-0,19908
E_{LUMO}a.u	-0,05924	-0,04692
$\Delta E=E_{LUMO}-E_{HOMO}$a.u	0,1316	0,15216
Ionization Potential (I)a.u	0,19084	0,19908
Electron affinity(A) a.u	0,05924	0,04692
Global Hardness (η) a.u	0,0658	0,07608
Chemical potential (μ) a.u	-0,12504	-0,123
Electronegativity (χ)au	0,12504	0,123
Global Softness (*S*)a.u	7,5987	6,572
Electrophilicity (ω)a.u	0,118805	0,09942
dipole moment (Deb)	7.0974	6.9575

Table 3. Molecular properties of compound

Table 3: Global reactivity index.

The MEP mapping is very useful in the investigation of the molecular structures with their physicochemical property relationships. The potential increases in the order of red < orange < yellow < green < blue [42].The color shown in the MEP (Figure 7) red partially negative charge or electron rich; blue partially positive charge or electron deficient; yellow slightly electron rich region and light blue slightly electron deficient region, respectively. The regions with negative potential - 9.172 Kcal/mol are on the electronegative atoms (nitrogen and oxygen atom of the hydroxyl group). Positive region was found on the hydrogen atom of the imine group, offering a potential of 9.172 Kcal/mol on its surface, indicating that this site may most likely be involved in nucleophilic processes.

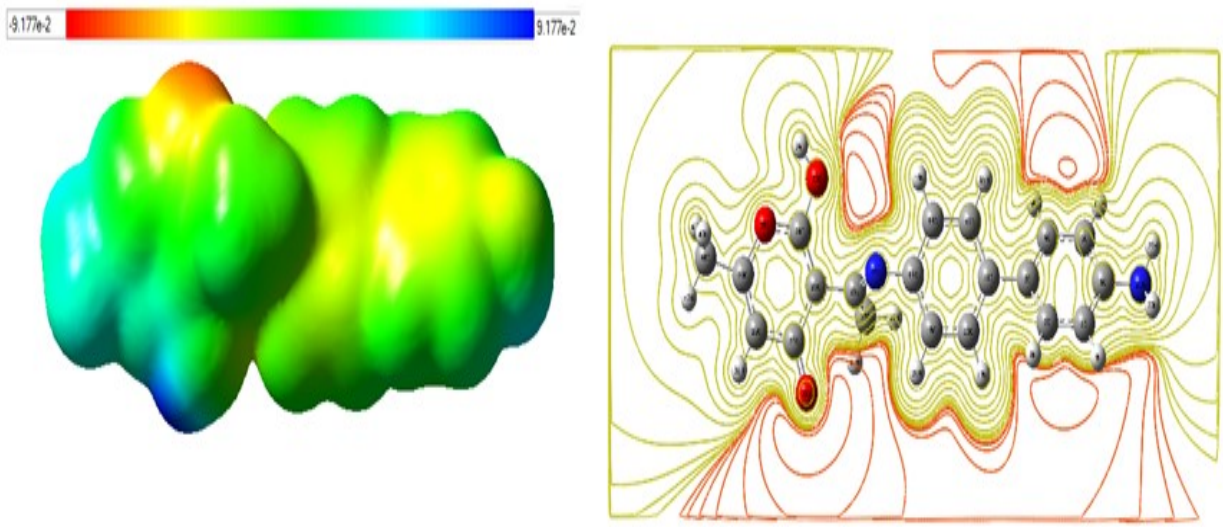

Figure.7. Molecular electrostatic potential (MEP) of compound

3. Conclusion

In the present work, new heterocyclic Schiff' base derivative, 3-[(1*Z*)-*N*-(4'-aminobiphenyl-4-yl)ethanimidoyl]-2-hydroxy-6-methyl-4*H*-pyran-4-one was synthesized and characterized by X-ray

diffraction, FT-IR and UV–Visible spectra. The compound crystallizes in monoclinic crystal system in C 2/c space group, unit cell parameters a=14.175(2), b=5.736(2) and c=21.150(2) A° andα =90°, β=107.5(6)°, ɣ=90°and Z=4. Hirshfeld surface was generated and analyzed in order to establish a quantitative insight into the intermolecular interactions. Density functional theory has been successful in providing insights into the chemical reactivity and selectivity in terms of global parameters, in order to predict the reactive sites for electrophilic and nucleophilic attacks in both molecules, MEP´s were calculated in the optimized geometry

Referances

[1]H.Schiff, (1864)MittheilungenausdemUniversitätslaboratorium in Pisa: EineneueReiheorganischerBasen. Justus LiebigsAnnalen der Chemie, vol 131, pp.118 119.

http://dx.doi.org/10.1002/jlac.18641310113

[2] B. Pedras, L. Fernandes, E. Oliveira, L. Rodríguez, M. Manuela M. Raposo, J. L. Capelo, C. Lodeiro(2009),Synthesis, characterization and spectroscopic studies of two new schiff-basebithienyl pendant-armed 15-crown-5 molecular probes; Inorganic Chemistry Communications, vol12, no 279-85

;https://doi.org/10.1016/j.inoche.2008.11.007

[3] L. Mishra, S. K. (2007). Dubey,Emission switching of ferrocenyl Schiff bases and a representative ruthenium complex in alkaline DMSO: Absorption, electrochemical and microstructural studies, Spectrochim. Acta, Part A, vol68,pp 364-368;

https://doi.org/10.1016/j.saa.2006.12.002

[4] K. Bhat, K.J. Chang, M.D. Aggarwal, W.S. Wang, B.G. Penn, D.O. Frazier, (1996),Synthesis and characterization of various Schiff bases for non-linear optical applications, Mater. Chem. Phys.vol 44,pp261-266:

https://doi.org/10.1016/0254-0584(96)80066-6

[5I. Finar, vol 2: Organic Chemistry, 5th ed., Longman, London, (1973).

[6] G. Ceyhan, M. Tümer, M. Köse, V. McKee, S. Akar,(2012) Structural characterization, luminescence and electrochemical properties of the Schiff base ligandsJournal of Luminescence.vol132, pp2917-2928

https://doi.org/10.1016/j.jlumin.2012.05.013

[7]YaliLuo, Shoucun Zhang, Yunxiang Ma, Wei Wang and Bien Tan, (2013),Microporous organic polymers synthesized by self-condensation of aromatic hydroxymethyl monomers, Polymer. Chimestry,vol. 41, pp126-1131.

https://doi.org/10.1039/C2PY20914D.

[8]W.AlZoubi, Abbas Ali Salih Al-Hamdani, MosabKaseem,(2016), Synthesis and antioxidant activities of Schiff bases and their complexes, a reviewApplied Organometallic Chemistry, vol30, no 10,pp810-817

[9] M. Mohan, P. Sharma, M. Kumar (1986),Metal Complexes of 2,6_Diacetylpyridine Bis(thiosemicarbazone): their Preparation, Characterization and Antitumor Activity.InorganicaChimicaActa, vol125 pp9.-15,

.https://doi.org/10.1016/S0020-1693(00)85476-6

[10] G. Turan-Zitouni, Z.A. Kaplancikli, A.Özdemir, P. Cheval Let. (2007), Studies on 1,2,4-Triazole Derivatives as Potential Anti-Inflammatory Agents. Archiv der Pharmazie,vol 340pp 586-590.

https://doi.org/10.1002/ardp.200700134

[11] M.T.H Tarafder, A.Kasbollah, N.Saravanan,K.ACrouse, A.M.Ali, (2002) S-Methyldithiocarbazate and Its Schiff Bases: Evaluation of Bondingsand Biological Properties. Journal of Biochemistry, Molecular Biology and Biophysics, vol6 pp85.

https://doi: 10.1080/10258140290027207

[12]M. SahooBiswa, C. DindaSubas, R. Kumar BVV, P. Jnyanaranjan, S. BrahmkshatriyaPathik; (2014) Design, Green Synthesis, and Anti-Inflammatory Activity of Schiff Base of 1,3,4-oxadiazole Analogues. Letters in Drug Design &Discovery,vol 11,no 1, pp82-89.

[13]A. M. Asiri, S. A. Khan, H. M. Marwani, K. Sharma, (2013), Synthesis, spectroscopic and physicochemical investigations of environmentally benign heterocyclic Schiff base derivatives as antibacterial agents on the bases of in vitro and density functional theory. Journal of Photochemistry and Photobiology B.vol120 pp82-.89,

.https://doi.org/10.1016/j.jphotobiol.2013.01.007

[14] H. Kumar and R.PalChaudhary, (2010) Biological Studies of a Novel Azo Based Heterocyclic Schiff Base and Its Transition Metal Complexes.DerChemicaSinica,vol1, pp55.

[15] G. M. Sheldrick, (2015), Crystal structure refinement with SHELXL. ActaCrystallogr.CStruct. Chem., vol71, pp3–8.

https://doi.org/10.1107/S2053229614024218

[16]L.J. Farrugia. (2012) Win GX and ORTEP for Windows: an update. J. Appl. Crystallogr. ,vol45, pp849–854.

https://doi.org/10.1107/S0021889812029111

[17] K. Brandenburg, (1998) Diamond Version 2.0 Impact GbR, Germany, Bonn,

[18] M. A. Wolff, S.K., Grimwood, D.J., McKinnon, J.J., Turner, M.J., Jayatilaka, D. and Spackman. (2012)., Crystal Explorer 17.5University of Western Austr.

[19] J. F. Janak, V. L. Moruzzi, and A. R. Williams(1975)Ground-state thermomechanical properties of some cubic elements in the local-density formalism.Physical Review B12, pp1257

https://doi.org/10.1103/PhysRevB.12.1257

[20] SharmiliSilvarajoo, Uwaisulqarni M. Osman, Khadijah H. Kamarudin, MohdHasmizamRazali, HanisMohdYusoff, IrshadUlHaqBhat, MohdZulHelmiRozaini, YusnitaJuahir, (2020) Dataset of theoretical Molecular Electrostatic Potential (MEP), Highest Occupied Molecular Orbital-Lowest Unoccupied Molecular Orbital (HOMO-LUMO) band gap and experimental cole-cole plot of 4-(ortho-, meta- and para-fluorophenyl)thiosemicarbazide isomers; Data in Brief 32, pp106299.https://doi.org/10.1016/j.dib.2020.106299

[21] C.T. Lee, W. Yang &R.G.Parr, (1988).Development of the Colle-Salvetti correlation-energy formula into a functional of the electron density.Physical Review 37B,pp78

https://doi.org/10.1103/PhysRevB.37.785

[22] R .G. Parr, W.Yang, Density Functional Theory of Atoms and Molecules, Oxford University Press, New York, (1989).

[23] A. D. Becke, (1993).Perspective on Density-functional thermochemistry.III. The role of exact exchange.J. Chem, Phys,vol98, pp5648

https://doi.org/10.1007/s002149900065

[24] G.A. Petersson, M.A. Al-Laham, (1991), A complete basis set model chemistry. II. Open-shell systems and the total energies of the first-row atoms.J. Chem. Phys. vol94, pp6081

https://doi.org/10.1063/1.460447

[25] G.A. Petersson, A. Bennett, T.G.Tensfeldt, M.A. Allaham, W.A.Shirley,J.Mantzaris,(1988).Kernel based quantum machine learning at record rate: Many-body distribution functionals as compact representationsJ. Chem. Phys., vol89, pp2193

https://doi.org/10.1063/1.455064

[26]H.Keypour, M. Mahmoudabadi, A. Shooshtari, M. Bayat, E. Soltani, R. Karamian, S.H.M Farida; .(2020), Synthesis, spectral, theoretical and antioxidant studies of copper (II) and cobalt (III) macroacyclicSchiffbase complexes containing homopiperazinemoietiy. Chem. Data Coll, vol26, pp100354.

https://doi.org/10.1016/j.cdc.2020.100354

[**27**]M. NadeemArshad, A.M. Asiri, K.A. Alamry, T. Mahmood, M. AmjadGilani, K. Ayub, A. SalehBirinji, (2015), Synthesis, Crystal Structure, Spectroscopic and Density Functional Theory (DFT) Study of N-[3- anthracen-9-yl-1-(4-bromo-phenyl)-allylidene]-N-benzenesulfonohydrazine.SpectrochimicaActa Part A: Molecular and Biomolecular Spectroscopy.vol142 pp364-374

https://doi.org/10.1016/j.saa.2015.01.101

[28] Cindric M, Vrdoljak V, Novak TK, C´uric´ M, Brbot-SaranovicA, Kamenar B. (2004) Synthesis and characterization of two dehydroacetic acid derivatives and molybdenum(V) complexes: an NMR and crystallographic study. Journal of Molecular Structure,vol701pp111–118.

https://doi.org/10.1016/j.molstruc.2004.05.025

[29]Chalaca MZ, Figueroa-Villar JD.(2000),A theoretical and NMR study of the tautomerism of dehydroaceticacidJournal of Molecular Structure vol.554, pp225–23

https://doi.org/10.1016/S0022-2860(00)00674-8

[30]HafeezUllah ,Feroza Hamid Wattoo , Muhammad Hamid Sarwar Wattoo1, Muhammad Gulfraz(2012), Syed Ahmad Tirmizi, Sadia Ata, Abdul Wadood;: Synthesis, spectroscopic characterization and antibacterial activities of three Schiff bases derived from dehydroacetic acid with various substituted anilines. Turkish Journal of Biochemistry–Turk J Biochem]; vol37 no 4,pp 386–391

.https://doi: 10.5505/tjb.2012.32650

[31]Asad, M., Arshad, M.N., T.N., M.M. and Asiri, A.M..Chitosan Catalyzed Novel PiperidiniumDicoumarol: (2022), Green Synthesis, X-Ray Diffraction, Hirshfeld Surface and DFT Studies. Polymers, vol14pp1854.

https://doi.org/10.3390/polym14091854

[32]Minaeva, V., Karaush-Karmazin, N., Panchenko, O., Minaev, B. and Ågren, H. (2023) Hirshfeld and AIM Analysis of the Methylone Hydrochloride Crystal Structure and Its Impact on the IR Spectrum Combined with DFT Study. Crystals,vol 13, pp383.

https://doi.org/10.3390/cryst13030383

[33]J. Aihara, (1999) Reduced HOMO−LUMO Gap as an Index of Kinetic Stability for Polycyclic Aromatic Hydrocarbons, J. Phys. Chem. Vol103,pp7487–7495.

https://doi.org/10.1021/jp990092i

[34] Y. Ruiz-Morales, (2002), HOMO−LUMO Gap as an Index of Molecular Size and Structure for Polycyclic Aromatic Hydrocarbons (PAHs) and Asphaltenes: A Theoretical Study, J. Phys. Chem. Vol106pp 11283–11308.

https://doi.org/10.1021/jp021152e

[35] I. Fleming. J. Wiley, (1976). Frontier Orbitals and Organic Chemical Reactions, Sons LTD, Londonpp 879–880

[36]Peter Politzer, Jane S. Murray, (1996), Relationships between dissociation energies and electrostatic potentials of CNO2 bonds: applications to impact sensitivities; Journal of Molecular StructureVol376, pp 419-424

https://doi.org/10.1016/0022-2860(95)09066-5

[36] J. Seminario, (1996) Recent Developments and Applications of Modern Density Functional Theory, first ed., Elsevier,vol 4 pp800–806.

[38] T. Yesilkaynak, G. Binzet, F. Mehmet Emen, U. Florke, N. Kulcu, H. Arslan, (2010)Theoretical and experimental studies on N-(6-methylpyridin-2-yl-carbamothioyl)biphenyl-4- carboxamide, Eur. J. Org. Chem., vol1, no1,pp1-5, .

https://doi.org/10.5155/eurjchem.1.1.1-5.3

[39] L.Padmaja, C. Ravikumar, D. Sajan, I. Hubert, V. Jayakumar, G. Pettit, O. Faurskov, (2009) Density functional study on the structural conformations and intramolecular charge transfer from the vibrational spectra of the anticancer drug combretastatin-A2, J. Raman. Spectrosc, vol. 4 pp419–428.

https://doi.org/10.1002/jrs.2145

[40] C. Ravikumar, I.H Joe, V.S Jayakumar, (2008), Charge transfer interactions and nonlinear optical properties of push–pull chromophorebenzaldehydephenylhydrazone: A vibrational approach, Chem. Phys. Lett, vol 460 pp552–558.

https://doi.org/10.1016/j.cplett.2008.06.047

[41] N. Sheela, S. Muthu, S. Sampathkrishnan, (2014) Molecular orbital studies (hardness, chemical potential and electrophilicity), vibrational investigation and theoretical NBO analysis of 4-40 -(1H-1,2,4-triazol-1-yl methylene) dibenzonitrile based on abinitio and DFT methods, Spectrochim. Acta.A. vol120 pp237–251.

https://doi.org/10.1016/j.saa.2013.10.007

[42] K. Carthigayan, S. Xavier, S. (2015) Periandy. HOMO–LUMO, UV, NLO, NMR and vibrational analysis of 3-methyl-1- phenylpyrazole using FT-IR, FT-RAMAN FT-NMR spectra and HF-DFT computational methods, Spectrochim. Acta.A. vol142 pp350–363.https://doi.org/10.1016/j.saa.2015.02.035